Appears in *Proceedings of IJCNN 2011*, IEEE Press

Perturbation Theory for Stochastic Learning Dynamics

Todd K. Leen and Robert Friel

***Abstract*— On-line machine learning and biological spike-timing-dependent plasticity (STDP) rules both generate Markov chains for the synaptic weights. We give a perturbation expansion (in powers of the learning rate) for the dynamics that, unlike the usual approximation by a Fokker-Planck equation (FPE), is rigorous. Our approach extends the related system size expansion by giving an expansion for the *probability density* as well as its moments. Applied to two observed STDP learning rules, our approach provides better agreement with Monte-Carlo simulations than either the FPE or a simple linearized theory. The approach is also applicable to stochastic neural dynamics.**

I. Introduction

BOTH on-line machine learning algorithms, and adaptation in many neural networks mediated by spike-timing-dependent plasticity (STDP) are stochastic processes described by a Markov process. While average dynamics may describe much phenomena, the fluctuations inherent in noisy learning create scatter around the average. This variability affects the accuracy with which a circuit can carry out its task. This is well-appreciated in on-line learning applied to adaptive filter theory [1][1]. A complete account of the effects of a noisy learning system specifies the time evolution of the *probability density* for the synaptic weights.

Unfortunately, the master or Chapman-Kolmogorov equations [3] for the evolution of the probability density are usually intractable. The most common approach is to use, in their place, a Fokker-Planck equation (FPE) [3][4] to describe the dynamics. The FPE has been successfully applied to both machine [5][6][7] and biological learning [8][9][10][11]. Despite its utility, its adoption is not theoretically well-justified. Van Kampen argues strongly against adopting a nonlinear FPE (unless rigorously derived by a proper limiting procedure), saying of its solutions that "any features they contain beyond that [predicted by linear drift and constant diffusion] are spurious" [12, p.272] Nonetheless, an FPE with nonlinear drift or non-constant diffusion (not rigorously derived) often gives good results.

The issue is not that the FPE is never a useful approximation, but rather that there is not a way to use it as the zeroth-order approximation to a complete perturbation expansion [13], which would enable one to make corrections to its predictions and discuss its domain of applicability. Van Kampen [12] derived his system-size expansion as a rigorous alternative to the FPE. However it is under-used and poorly understood, in part because the development is difficult [14]. Furthermore the method does not give higher-order corrections to the *probability density*, which would provide useful visualization.

We give here a perturbation approach appropriate for machine and STDP learning, and for neurodynamics. We give a clear, simple development that supplies the *density* as well as its moments. We use a discrete-time approach, which may be more appropriate than continuous-time dynamics for comparison with transients in learning experiments and simulations.

We apply our expansions to two observed STDP learning rules: the antisymmetric Hebbian learning observed by Bi and Poo [15] and modeled by van Rossum [8], and the anti-Hebbian learning observed in weakly electric fish by Bell et al. [16], and first modeled by Roberts et al. [17]. For the Hebbian rule, we compare equilibrium densities predicted by our perturbation expansion with those from the FPE, and with histograms from Monte-Carlo simulations. In parameter regimes for which the FPE does not agree with the simulations, the perturbation expansion shows good agreement. For the electric fish anti-Hebbian rule, we compare moments of the equilibrium densities predicted by our perturbation expansion with those from the FPE and from a linearized theory. The results show large differences between the theoretical methods, with the perturbation expansion in far better agreement with simulations.

In Section IIA we develop the fundamental dynamics for STDP including the equations of motion for the probability density on the synaptic weights. We develop our perturbation solution to those equations in Section IIB. In Section III we apply the methods to two observed STDP learning rules and compare predictions with the FPE.

II. Noisy Learning

A. Ensemble Dynamics

Machine learning via on-line algorithms and many observed biological learning rules mediated by STDP can both be described by learning rules of the form

$$w_{t+1} \;=\; w_t \;+\; \eta\, h(w_t, \psi_t) \tag{1}$$

where w_t is the synaptic weight at time-step t, η is the learning rate (constant for this discussion), $h(\cdot)$ is the learning rule, and ψ is a random variable giving rise to the randomness of the dynamics. In the machine learning context, ψ_t might be the example chosen from the data to feed into the algorithm at time step t [18]. In STDP, randomness can arise out of fluctuations in the relative timing

Todd K. Leen and Robert Friel are with the Dept. of Biomedical Engineering at OHSU (email: tleen@bme.ogi.edu). We thank Patrick Roberts for helpful conversation and the reviewers for useful comments. This work was supported by NSF grant IIS-0812687.

[1]Similarly, the dynamics and function of neural *activity* can be described in mean terms by firing rates. However this treatment neglects the role of correlated firing [2]

between the pre-synaptic and post-synaptic events [17][19], or by noise present in the synaptic changes even at fixed relative timing [8]. The vector variable ψ_t collectively carries all these effects.

The learning rule (1) generates a Markov process on w; the weight w_{t+1} depends only on the weight w_t and the probability of the transition $w_t \to w_{t+1}$. The probability density for the weights thus evolves according to the Chapman-Kolmogorov equation [3]

$$P(w, t+1) \;=\; \int P(w', t)\, W(w' \to w)\, dw' \qquad (2)$$

where $W(w' \to w)$ is the probability of making the transition from w' to w in one time step. The transition probability for *fixed* ψ is a delta function satisfying the learning rule (1), and we obtain the unconditional transition probability by taking its expectation with respect to ψ

$$\begin{aligned} W(w' \to w) &= E_\psi[W(w' \to w|\psi)] \\ &= E_\psi\left[\, \delta(w - w' - \eta\, h(w', \psi))\, \right] \quad . \end{aligned} \qquad (3)$$

The Kramers-Moyal (KM) expansion [3] of the Chapman-Kolmogorov equation (2) serves as the starting point for our perturbation treatment, and for comparison with the commonly-adopted Fokker-Planck equation (FPE). To derive the KM expansion, substitute the transition probability (3) into the Chapman-Kolmogorov equation (2), multiply both sides by a smooth test function $\kappa(w)$ of compact support (but otherwise *arbitrary*), and integrate over w. Then Taylor expand the result about $\eta = 0$. Finally, integrate by parts to take all derivative operators off $\kappa(w)$ to find

$$P(w, t+1) - P(w, t) = \sum_{j=1}^{\infty} \frac{(-\eta)^j}{j!}\, \partial_w^j\, (\alpha_j(w)\, P(w, t)) \quad . \qquad (4)$$

Here ∂_w^j denotes the j^{th} partial derivative with respect to w, and the *jump moments* are

$$\alpha_j(w) \;=\; E_\psi\left[\, h^j(w, \psi)\,\right] \quad . \qquad (5)$$

The first jump moment $\alpha_1(w)$, called the *drift coefficient*, captures the average dynamics[2]. The second jump moment $\alpha_2(w)$, called the *diffusion coefficient*, describes the propensity of the system to spread out over the configuration space.

The KM expansion (4) is usually intractable. The common procedure is to retain only the first two terms, the FPE

$$\begin{aligned} P(w, t+1) - P(w, t) = &-\eta\, \partial_w\, (\alpha_1(w)\, P(w, t)) \\ &+ \frac{\eta^2}{2} \partial_w^2\, (\alpha_2(w), P(w, t)) \quad . \end{aligned} \qquad (6)$$

The truncation of the KM expansion to the FPE is convenient and widely-used. However it is only strictly justified when arrived at by a limiting procedure in which the higher order jump moments $\alpha_3, \alpha_4, \ldots$ necessarily vanish. In machine and biological learning systems (and in the treatment of fluctuations in neural activity), the truncation is generally not justified.

[2]Indeed, if $\alpha_1(w)$ is *linear*, then the motion of the system mean follows $E[w](t+1) = E[w](t) + \eta\alpha_1(E[w](t))$.

Instead of adopting the FPE equation, we develop a perturbation expansion for the dynamics of $P(w, t)$. Our treatment follows the roots of van Kampen's system size expansion, and so gives the same results for the moments. However we give a much clearer development than previously available, and our approach provides approximations for the *density* as well as the moments.

Following van Kampen, we decompose the weight trajectory w_t into the sum of a deterministic and a fluctuating piece

$$w_t \;=\; \phi_t \;+\; \sqrt{\eta}\, \xi_t \qquad (7)$$

where ϕ_t is the deterministic piece and ξ_t are the fluctuations. In analogy with a simple random walk (and in the spirit of the central limit theorem) we have assumed that the *variance* of w at late times t scales *linearly* with the step size η, hence the $\sqrt{\eta}$ multiplying ξ. This scaling assumption is ultimately verified by confirming that the lowest order contribution to the variance of ξ is indeed independent of η.

We want to retain a discrete-time dynamical description, which is more appropriate for learning rules than continuous-time versions. So our development departs significantly from that in previous literature (for example as given by Gardiner [3]). To extract the dynamics of the deterministic piece, we substitute the decomposition in Eqn. (7) into the learning rule of Eqn. (1) leaving

$$\begin{aligned} \phi_{t+1} + \sqrt{\eta}\; \xi_{t+1} \;=\; \phi_t \;+\; \sqrt{\eta}\, \xi_t \\ + \eta\, h(\phi_t + \sqrt{\eta}\, \xi_t, \psi_t) \quad . \end{aligned} \qquad (8)$$

Next, expand the last term on the right-hand side of Eqn. (8) in powers of $\sqrt{\eta}$ and take the expectation of both sides with respect to ψ. Extracting the pieces of the result that are *independent of* ξ_t yields the equation for the deterministic trajectory

$$\phi_{t+1} \;=\; \phi_t \;+\; \eta\, \alpha_1(\phi_t) \quad . \qquad (9)$$

Finally, to obtain the equation of motion for the fluctuations, substitute Eqn. (9) into Eqn. (8) yielding

$$\begin{aligned} \xi_{t+1} &= \xi_t \;+\; \sqrt{\eta}\, (\, h(\phi_t + \sqrt{\eta}\, \xi_t, \psi) - \alpha_1(\phi_t)\,) \\ &\equiv \xi_t \;+\; \sqrt{\eta}\, H(\phi_t + \sqrt{\eta}\, \xi_t, \psi_t) \quad , \end{aligned} \qquad (10)$$

where we have defined the *fluctuation learning function*

$$H(w,\, \phi, \psi) \;\equiv\; h(w,\, \psi) - \alpha_1(\phi) \quad . \qquad (11)$$

We can obtain a KM expansion for the evolution of the probability density on ξ by steps analogous to those leading to Eqn.(4). The result is

$$\begin{aligned} P(\xi, t+1) - P(\xi, t) \;=\; \\ \sum_{j=1}^{\infty} \frac{(-\eta)^{j/2}}{j!}\, \partial_\xi^j\, (A_j(\phi_t + \sqrt{\eta}\xi)\, P(\xi, t)) \end{aligned} \qquad (12)$$

where the *fluctuation jump moments* are

$$A_j(w, \phi) \;=\; E_\psi\left[\, H^j(w, \phi, \psi)\,\right] \quad . \qquad (13)$$

(Compare Equations (5) and (13).) We complete the derivation by expanding the jump moment on the right-hand side of Eqn.(12) in powers of $\sqrt{\eta}$ and re-arranging terms to find

$$P(\xi,t+1)-P(\xi,t) \;=\; \sum_{k=2}^{\infty}\sum_{j=1}^{k}\frac{(-1)^j}{j!(k-j)!}\,\eta^{k/2}\,A_j^{(k-j)}\,\partial_\xi^j\left(\xi^{k-j}\,P(\xi,t)\right) \quad (14)$$

where we have used $A_1(\phi)\equiv 0$, and defined

$$A_j^{(m)} \;\equiv\; \partial_w^m A_j(w,\phi)\big|_{w=\phi_t} \quad , \qquad (15)$$

the coefficients of the expansion of the j^{th} jump moment about ϕ_t. Equations (9) and (14) together provide a complete description of the dynamics. The right-hand side of Eqn. (14) is identical to that in the continuous-time system size expansion [3] apart from the definition of the jump moments.

B. Perturbation Solution for the Density and Moments

Here we give simple and direct perturbation expansions for the probability density of the fluctuations, and its moments. Equation (14) for the fluctuation density is of the form

$$P(\xi,t+1)-P(\xi,t) \;=\; \eta\left(\,L_0+\eta^{1/2}\,L_1+\eta\,L_2+\ldots\right)\,P(\xi,t) \qquad (16)$$

where each L_i is a sum of differential operators of order $1,2,\ldots(i+2)$. For reference, the first two are

$$L_0 f(\xi) \;=\; -A_1^{(1)}\partial_\xi(\xi\,f)+\frac{1}{2}A_2^{(0)}\,\partial_\xi^2\,f \qquad (17)$$

$$L_1 f(\xi) \;=\; -\frac{1}{2}A_1^{(2)}\partial_\xi(\xi^2 f)+\frac{1}{2}A_2^{(1)}\partial_\xi^2(\xi f) -\frac{1}{3!}A_3^{(0)}\partial_\xi^3 f \quad . \qquad (18)$$

For the remainder of the paper, we confine attention to *equilibrium* solutions for which $\phi_{t+1}=\phi_t$, and $P(\xi,t+1)=P(\xi,t)$. We assume that there are no constraints bounding the values of the weights and restrict attention to equilibrium solutions that are peaked up around asymptotically-stable fixed points ϕ_* of the deterministic trajectory (9)

$$\alpha_1(\phi_*)=0 \qquad (19)$$

$$-2<\eta\alpha_1^{(1)}(\phi_*)<0 \quad , \qquad (20)$$

where the first condition establishes the fixed point, and the second its asymptotic stability [20]. In what follows, we assume that $\phi=\phi_*$. Note that from Eqns. (11) and (19), at $\phi=\phi_*$, $H=h$. It follows from Eqns. (5) and (13) that $A_j(w)=\alpha_j(w)$ at $w=\phi_*+\eta\xi$. Consequently the equilibrium of the discrete-time and continuous-time systems are identical, as one would expect. Finally, at equilibrium, the left side of Eqn. (16) is zero. Henceforth we drop the time-dependence.

To develop a perturbation expansion for the equilibrium density, we write

$$P(\xi) \;=\; P^{(0)}(\xi)+\eta^{1/2}P^{(1)}(\xi)+\eta\,P^{(2)}(\xi)\,+\,\ldots \qquad (21)$$

where the $P^{(k)}(\xi)$ are unknown. This decomposition, along with the operator expansion in Eqn. (16), are the *critical elements* that provide a clear development for the approximations to the density and its moments.

To solve for the $P^{(k)}$ we substitute the series in Eqn. (21) into Eqn. (16) (with the latter's left-hand side set to zero at equilibrium). Since the resulting equation must hold regardless of the value of η, it must be true that the terms of equal order in η separately vanish. Hence we obtain a succession of equations

$$L_0\,P^{(0)}(\xi) \;=\; 0 \qquad (22)$$

$$L_0\,P^{(1)}(\xi) \;=\; -L_1\,P^{(0)} \qquad (23)$$

$$L_0\,P^{(2)}(\xi) \;=\; -L_1\,P^{(1)}(\xi)\;-\;L_2\,P^{(0)}(\xi) \quad . \qquad (24)$$

and so on.

The zeroth-order density $P^{(0)}(\xi)$ satisfies Eqn. (22), which carries the *linear* part of the drift and the *constant* part of the diffusion coefficients — see Eqn. (17). This describes the equilibrium of an Ornstein-Uhlenbeck process [3]. The solution is a Gaussian with mean zero and variance

$$\sigma_0^2 \;=\; \frac{\alpha_2(\phi_*)}{2|\alpha_1^{(1)}(\phi_*)|} \quad . \qquad (25)$$

This is the lowest order (so-called *linear noise approximation*) piece of van Kampen's system size expansion. By Eqn. (21), in the limit $\eta\to 0$ the density is dominated by $P^{(0)}(\xi)$. Thus the equilibrium solution (peaked up about an asymptotically-stable fixed point ϕ_*) for *any learning rule* approaches this Gaussian at low learning rates. Finally, since this lowest order approximation to the variance (25) is *independent* of η, the scaling of fluctuations in the original decomposition is justified, as per the paragraph immediately following Eqn. (7).

1) Perturbation Corrections to the Density: To obtain the higher-order corrections to the density $P^{(i)}(\xi),\ i=1,2,\ldots$ we require the eigenfunctions of L_0 and its adjoint $L_0^\dagger$

$$L_0\,f_k(\xi) \;=\; \lambda_k\,f_k(\xi) \qquad (26)$$

$$L_0^\dagger\,g_k(\xi) \;=\; \lambda_k\,g_k(\xi)\;,\quad k=0,1,2,\ldots \quad . \qquad (27)$$

The $g_k(\xi)$ are Hermite polynomials, and the $f_k(\xi)$ are Hermite polynomials times a Gaussian (harmonic oscillator wave functions). The first of these is the zeroth-order density $P^{(0)}(\xi)=f_0(\xi)$. The eigenvalues are $\lambda_k=-k|\alpha_1^{(1)}|$. The two sets of functions form a bi-orthogonal set $(g_j,f_k)=\delta_{jk}$ under the standard $\mathcal{L}_2$ inner product [3, Section 5.2].

To find the first order (in $\eta^{1/2}$) correction to the density, we expand it as linear combination of eigenfunctions

$$P^{(1)}(\xi) \;=\; \sum_{j=1}^{\infty} a_j\,f_j(\xi) \quad . \qquad (28)$$

To find the coefficients a_j, substitute this expansion into Eqn. (23), take the inner product of both sides with g_k and use the bi-orthogonality. The result is

$$P^{(1)}(\xi) \;=\; -\sum_{k=1}^{\infty}\frac{1}{\lambda_k}\left(g_k, L_1P^{(0)}\right)\,f_k(\xi) \quad . \qquad (29)$$

With this correction in hand, the next is found following the same procedure on Eqn. (24). The result is

$$P^{(2)}(\xi) \;=\; -\sum_{k=1}^{\infty} \frac{1}{\lambda_k} \Big(g_k, L_1 P^{(1)} + L_2 P^{(0)} \Big) \, f_k(\xi) \;\; . \quad (30)$$

Calculating the corrections to the density requires evaluating inner products of the form $(g_k,\, L_p f_j)$. To do so, we use the adjoint of L_p to re-write them as $(g_k,\, L_p f_j) \;\equiv\; (L_p^\dagger g_k, f_j)$. Recall that the g_k are Hermite polynomials of order k, and $L_p^\dagger$ contains terms of the form $\xi^n \partial_\xi^m$. Using the well-known recursion relations for the Hermite polynomials [21, for example] we can write $L_p^\dagger g_k$ as a finite sum of several different Hermite polynomials $g_l(\xi)$. The bi-orthogonality condition $(g_n, f_l) = \delta_{n,l}$ allows one to complete the calculations easily. The inner products $\big(L_p^\dagger g_k,\, f_j\big)$ are nonzero over only a finite set of the eigenfunctions f_j; hence the sums over k in Eqns. (29), (30), and the higher-order analogs terminate after a finite number of terms.

It is important to note that perturbation expansions are typically asymptotic but not convergent [22]. Hence, the accuracy of our expansion improves as $\eta \to 0$, but retaining more terms in the perturbation expansion (21) may not improve its accuracy at non-zero η. This is typical for perturbation expansions.

2) Perturbation Corrections to the Moments: The lowest order solution $P^{(0)}(\xi)$ is a Gaussian with mean zero and variance given by Eqn. (25). The corrections to any of the moments can be calculated order-by-order in $\eta^{1/2}$ as follows. We define a perturbation series for the k^{th} moment by multiplying both sides of Eqn. (21) by ξ^k and integrating to obtain

$$M_k(\eta) \;=\; M_k^{(0)} + \eta^{1/2} M_k^{(1)} + \eta M_k^{(2)} + \cdots \quad (31)$$

where the n^{th} order correction to the k^{th} moment is

$$M_k^{(n)} \;\equiv\; \int \xi^k \, P^{(n)}(\xi) \, d\xi \;\; .$$

Now return to the succession of perturbation equations (22)–(24). Multiply both sides of each by ξ^k and use the definition of the adjoint of L_n to move their action off the Ps and onto the ξ^k. This leaves the set of equations

$$0 \;=\; \int P^{(0)} L_0^\dagger \xi^k \, d\xi \quad (32)$$

$$0 \;=\; \int P^{(1)} L_0^\dagger \xi^k + P^{(0)} L_1^\dagger \xi^k \, d\xi \quad (33)$$

$$0 \;=\; \int P^{(2)} L_0^\dagger \xi^k + P^{(1)} L_1^\dagger \xi^k + P^{(0)} L_2^\dagger \xi^k \, d\xi \quad (34)$$

and so forth. These yield a set of algebraic equations for the corrections to the moments as follows. The terms $L_p^\dagger \xi^k$ reduce to polynomials with terms $\xi^{k+p}, \xi^{k+p-2}, \ldots, \xi^{\max[0,k-p-2]}$. Hence the integrals in Eqns.(32) –(34) are of the form

$$\int P^{(n)}(\xi) \; L_p^\dagger \xi^k \, d\xi \;\; = \;\; a_{k+p} M_{k+p}^{(n)} + a_{k+p-2} M_{k+p-2}^{(n)} + \cdots + a_{k-p-2} M_{i-p-2}^{(n)} \quad (35)$$

where the series terminates at $M_0^{(n)}$. One can verify that to obtain $M_k^{(n)}$ one needs only the moments $M_{k+i}^{(n-i)}$, $M_{k+i-2}^{(n-i)}$, $\ldots$, $M_{i-i-2}^{(n-i)}$, for $i = 0, 1, 2, \ldots n$. Thus the perturbation framework yields a set of *algebraic* equations that provide the equilibrium moments in increasing order of $\eta^{1/2}$. For completeness, we give the first few of these below.

The zeroth order density is a Gaussian with zero mean and variance (25). In *all* orders, the normalization of the perturbation density (21) is unity, reflected by the result $M_0^{(n)} = 0$, $n > 0$. The first few corrections are

$$\begin{aligned}
M_2^{(1)} &= M_1^{(2)} = M_3^{(2)} = 0 \\
M_1^{(1)} &= -\frac{\alpha_1^{(2)}}{2\alpha_1^{(1)}} \, M_2^{(0)}, \\
M_3^{(1)} &= -\frac{1}{3\alpha_1^{(1)}} \left(\frac{3}{2} \alpha_1^{(2)} M_4^{(0)} + 3\alpha_2^{(0)} M_1^{(1)} \right. \\
&\qquad \left. + 3\alpha_2^{(1)} M_2^{(0)} + \alpha_3^{(0)} \right) \\
M_2^{(2)} &= -\frac{1}{2\alpha_1^{(1)}} \left(\alpha_1^{(2)} M_3^{(1)} + \frac{1}{3} \alpha_1^{(3)} M_4^{(0)} \right. \\
&\qquad \left. + \alpha_2^{(1)} M_1^{(1)} + \frac{1}{2} \alpha_2^{(2)} M_2^{(0)} \right) \;\; . \quad (36)
\end{aligned}$$

One assembles the terms $M_k^{(0\ldots n)}$ into the series in Eqn. (31) and lastly forms the moments of the weight w from the original decomposition in Eqn. (7) $E[w^k] = E[(\phi_* + \eta^{1/2}\xi)^k] \;\; .$

We have implemented our perturbation expansions for the density functions and for the moments in the Mathematica[3] computer algebra language. This provides fast and accurate evaluation of the other-wise tedious expressions.

III. Biological Plasticity

We apply the methods from the last section to two observed biological STDP learning rules: antisymmetric Hebbian learning, and the anti-Hebbian learning observed in the electro-sensory lateral line lobe (ELL) of weakly electric fish. We give theoretical results for both the probability density function and its moments, and compare them with results from Monte-Carlo simulations.

A. Antisymmetric Hebbian Learning

Several researchers have observed antisymmetric Hebbian learning in which synapses are potentiated if the presynaptic spike precedes the post-synaptic spike, and depressed if the presynaptic spike follows the post-synaptic spike [15][23][24]. Van Rossum, Bi, and Turrigiano applied a nonlinear Fokker-Planck equation to model the equilibrium synaptic weight distribution in one such learning rule [8]. Their analysis draws on Bi and Poo's experimental results [15] for the particular learning rule form and modeling parameters.

[3] *Mathematica 7.0*, Wolfram Research Inc. 2008.

The learning rule used by van Rossum et al. [8] is

$$\begin{aligned} w_{t+1} &= w_t + \eta\, w_p(w_t, \delta t) \\ &= w_t + \eta(c_p + v\, w_t)\, e^{-\delta t/\tau},\ \delta t > 0 \\ w_{t+1} &= w_t + \eta\, w_d(w_t, v, \delta t) \\ &= w_t + \eta(-c_d\, w_t + v\, w_t)\, e^{\delta t/\tau},\ \delta t \le 0 \end{aligned} \quad (37)$$

where the first expression describes potentiation, and the second expression describes depression. In Eqn. (37), δt is the time of the post-synaptic spike minus the time of the synaptic event, c_p and c_d are constants determining the amount of potentiation and depression respectively, τ is the time constant for the exponential learning window, and v is zero mean Gaussian noise of variance σ_v^2 describing the experimentally-observed fluctuations. The multiplicative scaling factor η facilitates application of the perturbation analysis.

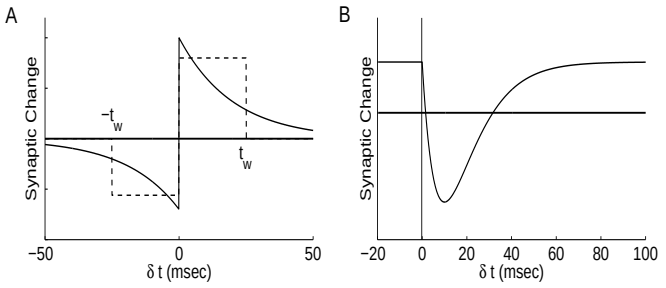

Fig. 1. A. Modeled time-dependence of learning in the model of van Rossum, and its approximation by a rectangular window function. B. Modeled time-dependence of electric fish anti-Hebbian learning rule (after Roberts [19]).

To make analytic progress, van Rossum et al. modify the learning rule by replacing each exponential lobe in Eqn. (37) with a unit height *rectangular* window functions of width t_w as shown in Figure 1A. With this simplification, the learning rule reduces to

$$\begin{aligned} w_{t+1} &= w_t + \eta\,(c_p + v\, w_t),\ 0 \le \delta t < t_w \\ w_{t+1} &= w_t + \eta\,(-c_d w + v\, w_t),\ -t_w \le \delta t < 0\ . \end{aligned} \quad (38)$$

Van Rosum et al. consider an integrate-and-fire neuron receiving background inputs plus incoming Poisson-distributed spikes on the single synapse w under study. This synapse undergoes depression with probability $p_d(w)$, the probability that the incoming spike arrives in the depression window $-t_w \le \delta t < 0$. It undergoes potentiation with probability $p_p(w)$, the probability that the incoming spike arrive in the potentiation window ($0 \le \delta t < t_w$. Since an input spike cannot influence the generation of an *earlier* post-synaptic spike, the depression probability is independent of w. However an incoming spike elevates the probability of a following post-synaptic spike, and so $p_p(w)$ increases with increasing w. The model captures this by taking $p_p(w) = p_d\,(1 + w/W_{tot})$, where W_{tot} is the effective synaptic weight of background inputs on the neuron. Van Rossum et al. assume that the synapse w contributes a minute fraction of the total input to the neuron, hence $w << W_{\rm tot}$. We follow that here[4], taking as they do

$$p_p = p_d \equiv p\ . \quad (39)$$

Under van Rossum's simplified model the required jump moments are easy to evaluate. Combining their definition Eqn. (5), the learning rule Eqn. (38), and the condition on the depression and potentiation probabilities Eqn. (39), one finds [25][26]

$$\begin{aligned} \alpha_n(w) &= p_p E_v[(c_p + v\, w)^n] \ +\ p_d E_v[(-c_d w + v\, w)^n] \\ &= p \sum_{k=0}^{\lfloor n/2 \rfloor} \binom{n}{2k} \sigma_v^{2k} (2k-1)!! \\ &\qquad \times \left(c_p^{n-2k} w^{2k} + (-c_d)^{n-2k} w^n\right) \end{aligned} \quad (40)$$

where $\lfloor q \rfloor$ is the largest integer equal to or less than q.

1) Equilibrium Density: As is typically done, van Rossum et al. truncate the Kramer-Moyal expansion (4) at the second term and use the FPE for the ensemble dynamics. For their model, the drift and diffusion coefficients are (using Eqn. (40))

$$\begin{aligned} \alpha_1(w) &= p\,(c_p - c_d\, w) \\ \alpha_2(w) &= p\,(\,c_p^2 + (c_d^2 + 2\sigma_v^2)\, w^2)\ . \end{aligned} \quad (41)$$

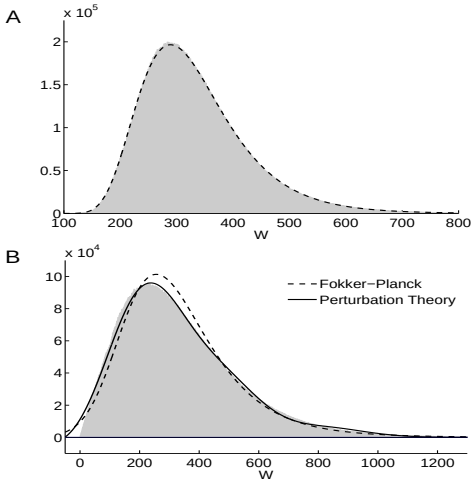

Fig. 2. Equilibrium distribution of weights from Monte-Carlo (shaded histogram) and as predicted by the FPE using (A) parameters from van Rossum et al., and (B) parameters for which the FPE fails. Also shown is the perturbation solution using terms through second order.

For a one-dimensional system (as here), the equilibrium distribution can be reduced to quadrature [4] with the result [8], [25]

$$\begin{aligned} P(w) &= \frac{K}{\alpha_2(w)} \exp\left(2 \int^w \frac{\alpha_1(w)}{\alpha_2(w)} dw\right) \\ &= K \frac{\exp\left(2 \arctan(\sqrt{2}\sigma' w/c_p)/\sigma'\right)}{(2\sigma'^2\, w^2 + c_p^2)^{\frac{2\sigma'^2 + c_d}{2\sigma'^2}}} \end{aligned} \quad (42)$$

where[5] $2\sigma'^2 \equiv 2\sigma_v^2 + c_d^2$, and we have set $\eta = 1$.

[4]We have derived the equilibrium moments without this assumption by a perturbation expansion in powers of $1/W_{tot}$ that we will discuss elsewhere.

[5]Van Rossum et al. further use $c_d^2 << \sigma_v^2$, as is appropriate for the biologically-observed parameters. Their solution follows from ours with the replacement $\sigma'^2 \to \sigma_v^2$.

Figure 2A shows the FPE equilibrium density (42) together with a histogram of weights from a Monte-Carlo simulation of the learning rule with 2×10^4 ensemble members sampled at 1,000 time steps. The parameters are the same as those used by van Rossum et al. $\eta = 1$, $c_p = 1$, $c_d = 0.003$, and $\sigma_v = 0.15$. The FPE solution matches the Monte-Carlo simulation quite well. The quadratic dependence of the diffusion coefficient α_2 on w (41) skews the theoretical distribution towards larger weights. The good fit of the FPE equilibrium for such a strongly-skewed distribution contradicts van Kampen's argument that such features arising from a non-linear FPE are "spurious" (see Section II-A).

At much higher values of c_p and c_d, the FPE ceases to model the distribution accurately since the contributions of the higher jump moments (α_3, $\alpha_4, \ldots$) become significant. Fig. 2B shows an example with $\eta = 1$, $c_p = 100$, $c_d = 0.3$, and $\sigma_v = 0.015$. The plot shows both the FPE (dashed curve) and the perturbation solution through second order (solid curve) for the equilibrium density. The FPE solution fails to capture the position of the peak properly. The perturbation solution does a better job since, through the operators L_1 and L_2 that occur in the solution (see Equations (29)–(30)), it takes into account contributions from α_3 and α_4. Hence the perturbation expansion makes effective use of information dropped by the Fokker-Planck truncation.

B. Anti-Hebbian Learning and Novelty Detection

Mormyrid weakly electric fish have several electrosensory modalities that they use for hunting and navigating. The fish emit a short electric organ discharge (EOD) (of duration $\sim$0.25 m-sec). Mormyromast electroreceptors on the surface of the skin sense the EOD field and their responses are processed centrally to detect distortions induced by nearby objects. A second system detects weak signals from animals (e.g. prey) using sensitive *ampullary* receptor organs.

The ampullary organs respond to the fish's own discharge with spike trains whose instantaneous rate resembles a damped (roughly) sinusoidal oscillations [27], persisting up to a hundred milliseconds. This response resembles ringing initiated by the EOD. The ringing response would grossly interfere with the fish's ability to detect weak signals from other organisms. To overcome this, processing in the electrosensory lateral line lobe (ELL) of the fish's brain builds a memory of the time course of the ampullary ringing response. The memory is actually an inverted copy, or *negative image*, of the ampullary response to the EOD. The negative image is combined with and nulls out the ampullary response to the EOD, allowing the brain to attend to signals from other oganisms. Thus the systems adapts to ignore the habitual signal arising from the fish's own EOD, allowing the organism to attend to potentially-important, novel signals. The negative image is modifiable on a time scale of minutes, so the fish can adjust to slow changes in the environment (for example changes in water conductivity) that would affect the ampullary response to the EOD [27][28][29].

Figure 3 shows a schematic of the system. The negative image is formed and combined with the ampullary input

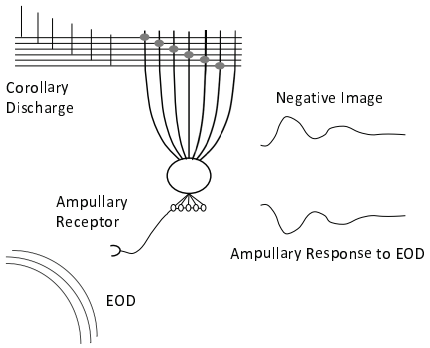

Fig. 3. Schematic showing ampullary receptor and corollary discharge inputs onto and MG cell, along with the ampullary response to the EOD, and it's negative image.

in *medium ganglion* (MG) cells in ELL. The MG cells have apical dendrites that receive inputs from parallel fibers originating outside ELL. These parallel fibers carry *corollary discharge* signals following the motor command that elicits the EOD. The corollary discharge signals on the parallel fibers arrive at MG cells with delays from 0 to about 100 m-sec following the EOD [17][27][28][29].

The mormyrid ELL was one of the first systems in which STDP was observed [30]. Plasticity at the parallel fiber synapses is responsible for forming and adapting the negative image. The plasticity is mediated by broad dendritic spikes in the MG cells This plasticity is sensitive to the time between the onset of the excitatory post-synaptic potentials (EPSP) resulting from the incoming parallel fiber spikes, and the broad dendritic spikes [17][30] (and references therein).

1) Average Dynamics and Negative Image: Roberts gave a model of ELL that predicts the formation and stability of the negative image using average learning dynamics [17][19]. Later work by Roberts, Williams, and Leen relaxed restrictions on the early models [31], and began to explore the stochastic dynamics of the model [32].

In the model formulated by Roberts and adapted by Williams et al. the MG cells receive signals originating at the ampullary receptors, and from the parallel fiber synapses. The resulting MG membrane potential is

$$U(x, w) = \gamma(x) + \sum_i w_i \, \mathcal{E}(x - x_i) \tag{43}$$

where x is the time since the last EOD, $\gamma(x)$ carries the effects of the ampullary inputs; w_i is the weight of the synapse from the i^{th} parallel fiber, carrying a corollary discharge spike delayed from the EOD by time x_i; and $\mathcal{E}(x - x_i)$ is the EPSP initiated at time x_i arising from the parallel fiber input to the i^{th} synapse. The second term on the right of Eqn. (43) carries the effect of the cascade of corollary discharge spikes, and through the synaptic weights w_i builds up the negative image. The EPSP time course is modeled as $\mathcal{E}(y) = \frac{y}{\tau^2} \exp -(y/\tau), \quad y \geq 0$, where τ is the time constant, and the factor $1/\tau^2$ normalizes the EPSP to unit area.

The learning rule is as follows. In the absence of a broad dendritic spike, EPSPs evoke a synaptic potentiation α. If

a broad dendritic spike occurs at time x the i^{th} synapse undergoes a change

$$\Delta w_i \;=\; \eta\,(\alpha - \beta L(x - x_i)) \tag{44}$$

where α and β are positive constants, $-L(x - x_i)$ is the learning function, and we have inserted the factor η to facilitate the perturbation expansion. The learning function is normalized to have unit area $\int L(x)dx = 1$. Figure 1(B) depicts the two components: the non-associative potentiation (grossly exaggerated), and the associative depression (following Roberts [19]).

The probability density for a broad dendritic spike occurring at time x after the EOD (equivalently the instantaneous broad spike rate) is modeled as a logistic sigmoid

$$f(x) \;=\; \frac{f_{\max}}{1 + \exp -\mu(U(x) - \Theta)} \tag{45}$$

where Θ is the broad spike threshold, and μ quantifies the effects of noise on spike generation through the slope of the sigmoid. We view Eqn. (45) as the instantaneous spike rate for a Poisson spike process. Williams et al. assume that at most one broad spike occurs during each EOD cycle and we adopt that assumption here as well. This is equivalent to a Poisson model with $f(x)$ always small enough so that the probability of more than one spike per EOD cycle is negligible. In follow-on work we relax this assumption.

Under these assumptions, the probability density for a broad dendritic spike in the interval $[x, x + dx]$, and the probability that there are zero spikes in the EOD cycle are

$$\text{Prob(spike in interval } [x, x + dx]) = f(x)\,dx \tag{46}$$

$$\text{Prob(no spikes)} = 1 - \int_0^T f(x)\,dx \tag{47}$$

respectively, where T is the EOD cycle length.

The average weight change in an EOD cycle is, from the expectation of Eqn.(44)

$$\langle \Delta w_i \rangle = \eta\,\alpha_{1i}(w) = \eta\left(\alpha - \beta \int_0^T f(x) L(x - x_i) dx\right) \tag{48}$$

Roberts [17][19] shows that with $L(x) = \mathcal{E}(x)$ (which holds approximately in the real system) there is a stable fixed point at which this average weight change is zero ($\alpha_{1i}(w) = 0$), and at this fixed point, the values of w are such that

$$U(x) \;=\; \gamma(x) + \sum_i w_i \mathcal{E}(x - x_i) \approx U_0 = \text{constant} \;. \tag{49}$$

That is, there is a stable fixed point for which a negative image of the ampullary signal $\gamma(x)$ is formed by the weighted sum of EPSPs initiated by the parallel fiber corollary discharges. At this negative image fixed point,

$$f(x) \;\approx f(U_0) \;\equiv\; f_0 \;=\; \alpha/\beta$$

having used the fact that $\langle \Delta w_i \rangle = 0$ at the fixed point, and $L(x)$ is normalized to unit area.

2) Beyond the Average Equations: Williams et al. [32] move beyond the average dynamics to explore the statistics of the equilibrium weight distribution. They proceed by *linearizing* the firing rate Eqn. (45) about the fixed point $U(x) = U_0$. This allows an *exact solution* for the moments of the equilibrium distribution (but not for the probability density). They address both a simplified model with a single synapse, and a full model with multiple synapses.

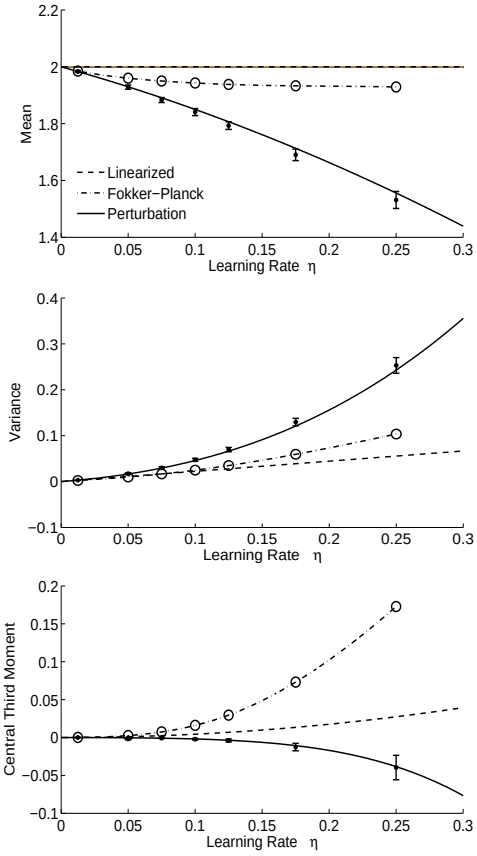

Fig. 4. First, second, and third central moments of the equilibrium distribution for ELL synaptic weights vs. learning rate. Shown are the moments calculated with the linearized theory (dashed), with the FPE (dot-dashed with open circles), with the perturbation analysis (solid), and from Monte-Carlo simulations (dots with $\pm 2\sigma$ confidence intervals).

We next apply our perturbation techniques from Section II-B to the single-synapse model, and compare our results with those from the linearized theory, from the FPE, and from Monte-Carlo simulations. The single parallel fiber input occurs at $x = 0$ and the membrane potential is taken to be

$$U(x) \;=\; U_0 + (w - w_*)\mathcal{E}(x)$$

so that the fixed point $\langle \Delta w \rangle = 0$, occurs at $w = w_*$ with $U(x) = U_0$. The jump moments follow from Eqn. (44) and the broad spike probabilities in Eqns. (45) and (47). We find

$$\alpha_n(w) \;=\; \alpha^n + \sum_{j=1}^{n} \alpha^{n-j}(-\beta)^j \left(\begin{array}{c} n \\ j \end{array}\right) \int_0^T f(x) L^j(x)\;. \tag{50}$$

Our perturbation methods require the derivatives of the jump moments at the fixed point $\partial_w^j \alpha_n(w*)$, and we evaluate the required integrals $\int \partial_w^j f(U(x, w_*) L^i(x) dx$ numerically.

Figure 4 shows the first three (central) moments of the equilibrium distribution as a function of the learning rate η. The plots show the moments predicted by the linearized theory, by the FPE (from numerical integration of the density), by our perturbation expansion, and from Monte-Carlo simulations (with $\pm 2\sigma$ confidence intervals). The perturbation results are clearly in better agreement with the Monte Carlo simulations than the linearized theory or the FPE for all but the smallest learning rates. Notice that both the FPE and the linearized theory give the *wrong sign* for the third central moment. The first moment was calculated to fifth order in perturbation, the second moment to seventh order, and the third moment to ninth order. At the highest learning rates the perturbation calculations of the mean and variance are beginning to break down; the theoretical predictions are at the very ends of the confidence limits. As discussed above, the series are asymptotic (more accurate as $\eta \to 0$) rather than convergent, and higher order perturbation calculations did *not* improve the agreement between the theory and the Monte-Carlo simulations[6].

IV. Discussion

The perturbation methods given here provide systematic tools for approximating the density and its moments for on-line machine and STDP biological learning, stochastic neural dynamics (recently addressed at lowest order with the system size expansion [2]. Our development gives a clear and simple order-by-order expansion that goes beyond the linear noise regime commonly retained from the system size expansion. Our implementation by computer algebra provides rapid and accurate evaluation. The moment equations generalize simply to multidimensional problems. Yet to be addressed are convergence of the series for cases where an exact solution (for the moments) exists, equilibria in bounded weight spaces, and STDP rules with triplet and quadruplet interactions.

References

[1] S. Haykin, *Adaptive Filter Theory, 2nd Edition*. Englewood Cliffs, NJ: Prentice Hall, 1991.

[2] M. A. Buice, J. D. Cowan, and C. C. Chow, "Systematic fluctuation expansion for neural network activity equations," *Neural Computation*, vol. 22, pp. 377–426, 2010.

[3] C. Gardiner, *Handbook of Stochastic Methods, 2nd Ed.* Berlin: Springer-Verlag, 1990.

[4] H. Risken, *The Fokker-Planck Equation*. Berlin: Springer-Verlag, 1989.

[5] R. Der and T. Villmannn, "Dynamics of self organized feature mapping," Universitat Leipzig, Inst. f. Informatik, Tech. Rep., 1993.

[6] G. Radons, "On stochastic dcynamics of supervised learning," *J. Phys. A*, vol. 26, pp. 3445–3461, 1993.

[6]The parameters are $\alpha = 0.003$, $\beta = 0.8$ [19], $\tau = 40$ms [31], $f\max = 0.0375 s^{-1}$, $\mu = 2$, and $T = 400$ms. The Monte Carlo has 4800 weights in the ensemble. The simulation was burned in for 2.5×10^4 EOD cycles and an additional 1×10^4 cycles (sub-sampled at the first zero of the autocorrelation function) were used to calculate the variances of the moment estimates.

[7] G. B. Orr and T. K. Leen, "Weight space probability densities in stochastic learning: II. Transients and basin hopping times," in *Advances in Neural Information Processing Systems, vol. 5*, Giles, Hanson, and Cowan, Eds. San Mateo, CA: Morgan Kaufmann, 1993.

[8] M. van Rossum, G. Bi, and G. Turrigiano, "Stable Hebbian learning from spike timing-dependent plasticity," *The Journal of Neuroscience*, vol. 20, pp. 8812–8821, 2000.

[9] H. Câteau and T. Fukai, "A stochastic method to predict the consequence of arbitrary forms of spike-timing-dependent plasticity," *Neural Computation*, vol. 15, no. 3, pp. 597–620, 2003.

[10] L. Zhu, Y. Lai, F. Hoppensteadt, and J. He, "Cooperation of spike timing-dependent and heterosynaptic plasticities in neural networks: A Fokker-Planck approach," *Chaos*, vol. 16, no. 2, p. 023105, 2006.

[11] B. Babadi and L. Abbott, "Intrinsic stability of temporally shifted spike-timing dependent plasticity," *PLoS Colmput. Biol.*, vol. 6, no. 11, p. e1000961, 2010, doi:10,1371/journal.pcbi.1000961.

[12] N. V. Kampen, *Stochastic Processes in Physics and Chemistry*. Amsterdam: North-Holland, 1981.

[13] T. M. Heskes and B. Kappen, "On-line learning processes in artificial neural networks," in *Mathematical Foundations of Neural Networks*, J. Taylor, Ed. Elsevier, 1993, pp. 199–233.

[14] E. W. Wallace, "A simplified derivation of the linear noise approximation," *Cornell University Library e-print archive*, vol. rXiv:1004.4280v4, 2010.

[15] Q. Bi and M. Poo, "Precise spike timing determines the direction and extent of synaptic modifications in cultured hippocampal neurons," *Journal of Neuroscience*, vol. 18, pp. 10 464–10 472, 1998.

[16] C. Bell, V. Han, Y. Sugawara, and K. Grant, "Synaptic plasticity in a cerebellum-like structure depends on temporal order," *Nature*, vol. 387, pp. 278–281, May 1997.

[17] P. D. Roberts and C. C. Bell, "Computational consequences of temporally asymmetric learning rules: II. Sensory image cancellation," *Journal of Computational Neuroscience*, vol. 9, pp. 67–83, 2000.

[18] R. O. Duda, P. E. Hart, and D. G. Stork, *Pattern Classification, 2nd Edition*. New York: John Wiley & Sons, 2001.

[19] P. D. Roberts, "Modeling inhibitory plasticity in the electrosensory system of mormyid electric fish," *Journal of Neurophysiology*, vol. 84, pp. 2035–2047, 2000.

[20] J. Guckenheimer and P. Holmes, *Nonlinear oscillations, Dynamical Systems, and Bifurcations of Vector Fields*. New York: Springer-Verlag, 1983.

[21] M. Abramowitz and L. S. (Eds.), *Handbook of Mathematical Functions*. U.S. Department of Commerce, National Bureau of Standards, 1972.

[22] C. M. Bender and S. A. Orszag, *Advanced Mathematical Methods for Scientists and Engineers, Asymptotic Methods and Perturbation Theory*. New York: Springer, 1999.

[23] H. Markram, J. Lubke, M. Fortscher, and B. Sakmann, "Regulation of synaptic efficacy by conicidence of postsynaptic AP's and EPSP's," *Science*, vol. 275, pp. 213–215, 1997.

[24] L. I. Zhang, H. W. Tao, C. E. Holt, W. A. Harris, and M. ming Poo, "A critical window for cooperation and competition among developing retinotectal synapses," *Nature*, vol. 395, pp. 37–42, 1998.

[25] F. A. Adrian, "Exact ensemble dynamics for spike-timing-dependent plasticity," Master's thesis, Department of Science & Engineering, OHSU, October 2008.

[26] T. K. Leen, F. A. Adrian, and R. Friel, "Exact and perturbation solutions for equilibria in spike-timing-dependent Hebbian learning," 2011, in preparation.

[27] C. Bell and T. Szabo, "Electroreception in mormyrid fish: Central anatomy," in *Electroreception*, T. Bullock and w. Heiligenberg, Eds. New York: Wiley, 1986, pp. 375–421.

[28] C. Bell, "Properties of a modifiable efference copy in an electric fish," *J. Neurophysiol.*, vol. 47, pp. 1043–1056, 1982.

[29] C. Bell, D. Bodznick, J. Montgomery, and J. Bastian, "The generation and subtraction of sensory expectations within cerebellum-like structures," *Brain Beh. Evol.*, vol. 50, pp. 17–31 (suppl. 1), 1997.

[30] C. Bell, V. Han, Y. Sugawara, and K. Grant, "Synaptic plasticity in a crebellum-like structure depends on temporal order," *Nature*, vol. 387, pp. 278–281, 1997.

[31] A. Williams, P. D. Roberts, and T. Leen, "Stability of negative-image equilibrium in spike-timing-dependent palsticity," *Physical Review E*, vol. 68, 2003.

[32] A. Williams, T. K. Leen, and P. D. Roberts, "Random walks for spike-timing-dependent plasticity," *Physical Review E*, vol. 70, 2004.